

## Solid-solid phase transitions and soft phonon modes in highly condensed Si

K. J. Chang and Marvin L. Cohen

*Department of Physics, University of California, Berkeley, California 94720*

*and Materials and Molecular Research Division, Lawrence Berkeley National Laboratory, Berkeley, California 94720*

(Received 28 January 1985)

The pseudopotential method is used to examine the structural transitions of Si from  $\beta$ -Sn to simple hexagonal (sh) to hexagonal close packed (hcp). The calculated transition pressures, transition volumes, and  $c/a$  ratios are in good agreement with the measured values. Furthermore, the phase-transition pressure from hexagonal close packed to face-centered cubic is predicted to be 1.2 Mbar. The phonon frequencies are also calculated with use of the frozen-phonon approximation for the  $\beta$ -Sn, sh, and hcp phases. For both the  $\beta$ -Sn and sh phases, pressure-sensitive soft phonon modes exist. These are the longitudinal optic mode at the Brillouin-zone center for  $\beta$ -Sn and the transverse acoustic mode at the Brillouin-zone boundary for sh in the [001] direction. These soft modes are most likely associated with the phase transformations from  $\beta$ -Sn to sh to hcp. The metallic sh phase has strong covalent interlayer bonding. This is opposite to the case for the graphite structure. The weak bonding in the hexagonal plane of the sh phase causes the soft transverse mode for this phase.

### I. INTRODUCTION

Although silicon is the most studied semiconductor, its high pressure metallic phases have only been actively examined in recent years. New developments in both theoretical and experimental techniques, i.e., the *ab initio* total-energy-pseudopotential method<sup>1</sup> and the diamond anvil technique,<sup>2</sup> have made it possible to investigate accurately the high-pressure behavior of materials, e.g., structural properties, solid-solid phase transitions, and dynamical properties.

It is well-known that Si under pressure transforms from the diamond to the metallic  $\beta$ -Sn structure at around 110 kbar.<sup>3-7</sup> In previous calculations,<sup>8,9</sup> the hexagonal close-packed (hcp), face-centered cubic (fcc), and body-centered cubic (bcc) structures have been examined as possible high pressure phases of Si. These calculations predicted the structural sequence cubic diamond to  $\beta$ -Sn to hcp for Si. The hcp phase of Si was later found to be stable at about 400 kbar in diamond cell experiments.<sup>5,7</sup> A rather interesting result of these experiments is that a simple hexagonal (sh) phase of Si also exists. This phase has been found at 160 kbar (Ref. 5) and 130 kbar (Refs. 6 and 7), and it transforms into the hcp phase at about 400 kbar. These experiments represent the first observations of a monoatomic system in the sh phase.

The sh phase contains 1 atom per unit cell and has been observed previously in alloys of Sn (Ref. 10) and in a Bi-In alloy.<sup>11</sup> This structure can be easily formed<sup>10</sup> from the  $\beta$ -Sn structure by displacing, along the tetragonal axis, one of the interpenetrating body-centered orthorhombic sublattices with a modification of the axial ratio (see Fig. 1). Similarly, the hexagonal close-packed structure can be created from the sh structure by sliding every other hexagonal plane with respect to its neighboring plane.

It is generally believed that the group-IV elemental and III-V compound semiconductors<sup>8,12</sup> transform into metallic phases with closely packed structures when they are

compressed. Si and Ge having tetrahedrally coordinated bonding favor the highly coordinated  $\beta$ -Sn phase (coordination number is 6) under pressure. The bcc, hcp, and fcc phases with coordination numbers 8, 12, and 12, respectively, appear at higher pressure. For the sh phase of Si, the  $c/a$  ratio was reported to be 0.936–0.947,<sup>5-7</sup> and thus in this phase the coordination number is 2. However, the effective coordination number of the sh phase is 8 since the axial ratio is close to 1. Using the coordination number<sup>8</sup> as a guide, it is expected that the sh phase of Si would be placed between  $\beta$ -Sn and either the bcc, hcp, or fcc phases at high pressure.

In this paper we present the results of *ab initio* pseudopotential calculations for investigating the origin of the structural stability for  $\beta$ -Sn, sh, and hcp Si under pressure. We also used the pseudopotential-total-energy scheme<sup>1</sup> to study the lattice dynamical behavior for each of the  $\beta$ -Sn, sh, and hcp structures. We have found that the phase transition from  $\beta$ -Sn to sh is caused by the soft longitudinal optic mode along the tetragonal axis of the  $\beta$ -Sn phase. For the sh phase, the bonding along the hexagonal axis appears to be stronger than the intraplane bonding. This behavior is opposite to the graphite structure of Si.<sup>13</sup> The transverse acoustic mode for the sh phase, in the [001] direction, is found to be soft compared to the longitudinal one. Furthermore, this transverse mode is sensitive to pressure and thus causes the phase transformation into the hcp structure. For the metallic  $\beta$ -Sn, sh, and hcp phases, the density of states appears to be higher than that of normal metals, suggesting that these metallic structures can be superconducting. Some preliminary results of this work were published earlier.<sup>14</sup> The results for the electronic properties,<sup>15</sup> the electron-phonon interaction, and the superconductivity<sup>16</sup> for  $\beta$ -Sn, sh, and hcp Si will appear elsewhere.

In Sec. II, we discuss the method used and the accuracy of the calculation. In Sec. III, the results of the calculations for the structural properties and the phonon fre-

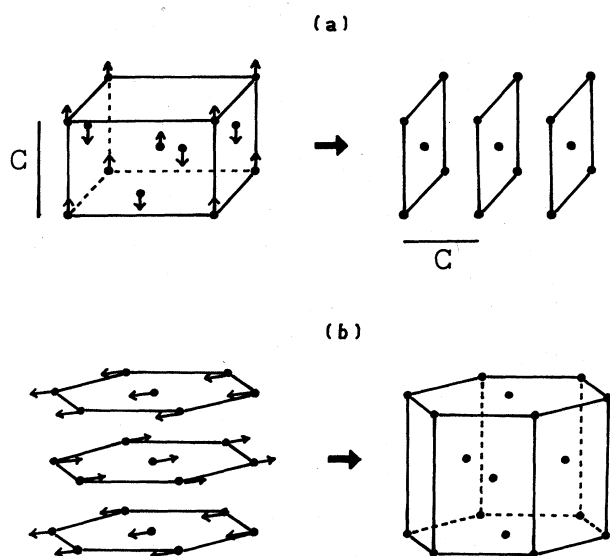


FIG. 1. Structural relationships between (a)  $\beta$ -Sn and sh and between (b) sh and hcp structures for Si. The arrows indicate the phonon displacements for (a) the LO( $\Gamma$ ) and (b) the TA( $A$ ) modes.

quencies are presented and discussed. The relation of the phase transitions to the phonon modes is also discussed. In Sec. IV concluding remarks are made.

## II. METHOD

The calculations are based on the pseudopotential-total-energy scheme.<sup>1</sup> The Wigner interpolation formula<sup>17</sup> is used to approximate the exchange and correlation functional. This total energy method using *ab initio* pseudopotentials has been successful in predicting the structural and dynamical properties for solids ranging from insulators<sup>8,12,18–20</sup> to metals.<sup>21,22</sup> The nonlocal *ab initio* pseudopotentials having *s*, *p*, and *d* symmetry are generated from the scheme proposed by Hamann, Schlüter, and Chiang.<sup>23</sup> The potentials used here were successfully employed in previous calculations for the structural<sup>8</sup> and dynamical<sup>20</sup> properties of Si.

The crystal total energies are calculated self-consistently in momentum space.<sup>24</sup> A plane-wave basis set with a kinetic energy cutoff up to 11.5 Ry is used to expand the wave function. For the summation over the Brillouin zone, a uniform grid of  $\mathbf{k}$  points is used for each phase, cubic diamond (CD), hexagonal diamond (HD),  $\beta$ -Sn, simple hexagonal, simple cubic (sc), hexagonal close-packed, body-centered-, and face-centered cubic structures. Since the diamond structure is an insulating phase, 10  $\mathbf{k}$  points are sufficient to obtain accuracy better than 0.5 mRy/atom. To compare the structural stability of the cubic and hexagonal diamond structures, we used 28  $\mathbf{k}$  points for CD and 27 for HD, respectively. These sets of  $\mathbf{k}$  points are larger than those used in previous calculation.<sup>8</sup> For the metallic phases of the  $\beta$ -Sn, sh, sc, hcp, bcc, and fcc structures, a large number of  $\mathbf{k}$  points is

necessary to represent the band overlap in  $\mathbf{k}$  space. Grids of 75, 150, 165, 146, and 140 sampling points in the irreducible Brillouin zone are chosen for  $\beta$ -Sn and hcp, sh, sc, fcc, and bcc, respectively. The resulting maximum error in the total energy is within 1 mRy/atom. The Gaussian's occupation for the electron states proposed by Fu and Ho<sup>25</sup> is also tested for the sh phase of Si. However, we found that this scheme is not effective for obtaining convergence of the total energy in condensed Si.

For the  $\beta$ -Sn, sh, and hcp structures which are not cubic, we optimized the total energies by varying  $c/a$  for a given volume. Since pressure delocalizes the bond charges, the  $c/a$  ratio is also relaxed under compression. The total energies are computed as a function of volume for various structural types, and then fitted to the Murnaghan's equation<sup>26</sup> of state. Thus, the ground state properties, such as lattice constants and bulk moduli, can be obtained. The calculated structural energies are highly accurate to distinguish the structural stability at various pressures, and to predict the transition pressure and volume for solid-solid phase transitions. Furthermore, the total energy change due to a distortion of crystal lattice can be used to calculate phonon frequencies within a few percent.

The calculations for the phonon frequency are done for the modes at high symmetry points in the Brillouin zone, e.g., the zone center and zone boundary phonons. For these phonon modes, the phonon waves are commensurate with the crystal lattice, and thus the cell contains twice as many atoms for zone boundary phonons while it has the same number of atoms at the zone center. Since the polarizations are completely determined by symmetry, the total energy for each mode can be evaluated with the use of the frozen-phonon approximation.<sup>20</sup> We estimate the phonon frequency from the energy difference between the undistorted and distorted lattices. The phonon modes are computed at  $\Gamma$  for the  $\beta$ -Sn and hcp structures and  $[00q_{\max}]$  points for the  $\beta$ -Sn, sh, and hcp phases. These phonon modes are of particular interest because some of them are related to the  $\beta$ -Sn $\rightarrow$ sh and sh $\rightarrow$ hcp phase transformations.

## III. RESULTS

### A. Solid-solid phase transitions

Recent observations<sup>5–7</sup> of the pressure-induced structural sequence (diamond $\rightarrow\beta$ -Sn $\rightarrow$ sh $\rightarrow$ hcp) for Si have confirmed the tendency to increase the coordination number under compression. A compression usually weakens the covalent bonding and the bond charges move to interstitial regions. In this case, the  $3d$  band moves downward.<sup>9</sup> This effect is normally represented by the decrease of the conduction band energies at the  $X$  point in the Brillouin zone for cubic crystals. As a consequence, the semiconducting diamond phase changes into metallic phases. On the other hand, the crystal favors structures with high coordination numbers when the bond is delocalized by a compression. For a fixed volume, the nearest-neighbor distance is enlarged if it is highly coordinated, and thus the charge density is less localized. As pressure increases, the electronic contribution to the total energy increases

while the core-core interaction (the Ewald term) energy decreases. Hence, the Ewald contribution at a compressed volume plays an important role in driving the phase transformation for the group-IV elemental semiconductors<sup>8</sup> into highly coordinated structures.

Figure 2 shows the results for the total energy calculations as a function of volume for several crystal structures. The sequence of the phase transition from diamond to  $\beta$ -Sn, to sh, and to hcp, is in good agreement with experiment. The calculations indicate that the  $\beta$ -Sn, sh, sc, bcc, hcp, and fcc structures are metallic phases. The densities of states at the Fermi energy for  $\beta$ -Sn, sh, and hcp phases are found to be sizable. The transition pressures and transition volumes are listed in Table I for the diamond to  $\beta$ -Sn,  $\beta$ -Sn to sh, sh to hcp, and hcp to fcc transitions. These are also compared with experiments and other calculations.

For the transition from diamond to  $\beta$ -Sn, the computed transition pressure of 93 kbar is consistent with a recently calculated value of 95 kbar by Yin<sup>27</sup> and the previous value of 99 kbar.<sup>8</sup> It is higher than another recently calculated value of 70 kbar.<sup>28</sup> The measured pressure varies

from 88 to 125 kbar.<sup>4-7</sup> However, analysis of these data suggests that 110 kbar could be considered as an appropriate value under hydrostatic pressures.<sup>29</sup> It was shown that nonhydrostatic stress lowers the transition pressure.<sup>7</sup> Therefore, all the calculations underestimate the transition pressure from the diamond to  $\beta$ -Sn structures.

The calculated pressure from  $\beta$ -Sn to sh is 120 kbar. The measured values are 160 (Ref. 5) and 132 (Refs. 6 and 7) kbar. For this transition, we consider this reasonably good agreement since the pressure is very sensitive to the number of  $k$  points used to represent the band overlap in  $k$  space and the type of the exchange and correlation functional.<sup>27</sup> Because of the proximity of the total energy curves between  $\beta$ -Sn and sh phases (see Fig. 2), the transition pressure represented by a common tangent between two  $E(V)$  curves has a variation of about 50 kbar when  $E(V)$  curves are changed by 0.5 mRy per atom. With 40  $k$  points for  $\beta$ -Sn and 75 for sh, the energy difference between two  $E(V)$  curves increases by 0.6 mRy/atom, and thus the pressure increases by 70 kbar. Two other calculations using the pseudopotential method have been reported, 149 (Ref. 27) and 143 (Ref. 28) kbar. However, it

TABLE I. Transition pressures and transition volumes for the cubic diamond to  $\beta$ -Sn,  $\beta$ -Sn to sh, sh to hcp, and hcp to fcc transitions. The volumes are all given as fractions of the measured equilibrium volume ( $20.002 \text{ \AA}^3/\text{atom}$ ) for the cubic diamond Si. The results are compared with experimental and other calculations.

Transition	$V_t (D)$	$V_t (\beta\text{-Sn})$	$V_t (\text{sh})$	$V_t (\text{hcp})$	$V_t (\text{fcc})$	$P_t (\text{kbar})$
$D \rightarrow \beta\text{-Sn}$						
Present calculation	0.931	0.719				93
Other calculation	0.915 <sup>a</sup>	0.707 <sup>a</sup>				95 <sup>a</sup>
	0.928 <sup>b</sup>	0.718 <sup>b</sup>				99 <sup>b</sup>
	0.926 <sup>c</sup>	0.719 <sup>c</sup>				100 <sup>c</sup>
	0.918 <sup>d</sup>	0.710 <sup>d</sup>				125 <sup>e</sup>
Experiment	0.911 <sup>f</sup>	0.706 <sup>f</sup>				113 <sup>f</sup>
	0.92 <sup>g</sup>					88 <sup>g</sup>
$\beta\text{-Sn} \rightarrow \text{sh}$						
Present calculation		0.707	0.692			120
Other calculation		0.678 <sup>b</sup>	0.661 <sup>h</sup>			143 <sup>h</sup>
		0.683 <sup>a</sup>	0.672 <sup>a</sup>			149 <sup>a</sup>
		0.69 <sup>g</sup>	0.673 <sup>f</sup>			160 <sup>g</sup>
Experiment						132–164 <sup>f</sup>
$\text{sh} \rightarrow \text{hcp}$						
Present calculation			0.603	0.556		410
Other calculation			0.580 <sup>a</sup>	0.538 <sup>a</sup>		
		0.608 <sup>c</sup>		0.563 <sup>c</sup>		410 <sup>c</sup>
Experiment			0.615 <sup>f</sup>	0.570 <sup>f</sup>		350–400 <sup>g</sup>
				0.54 <sup>f</sup>		360–420 <sup>f</sup>
$\text{hcp} \rightarrow \text{fcc}$						
Present calculation				0.465	0.456	1160
Other calculation				0.482 <sup>c</sup>		800 <sup>c</sup>

<sup>a</sup>Reference 27.

<sup>b</sup>Reference 8.

<sup>c</sup>Reference 9.

<sup>d</sup>Reference 34.

<sup>e</sup>Reference 4.

<sup>f</sup>References 6 and 7.

<sup>g</sup>Reference 5.

<sup>h</sup>Reference 28.

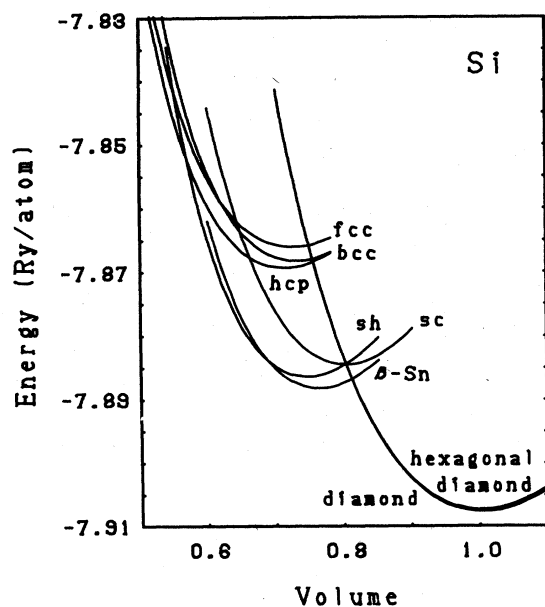


FIG. 2. The total structural energy versus the volume normalized by the calculated equilibrium volume in the diamond structure.

should be noticed that these numbers are obtained using a set of smaller number of  $k$  points for 143 kbar (40 for  $\beta$ -Sn and 60  $k$  points for sh) and using fixed values of  $c/a$  for both the  $\beta$ -Sn and sh phases for 149 kbar. We also tested the Gaussian occupation scheme for the electron states proposed by Fu and Ho.<sup>25</sup> This scheme was successful in getting the convergence faster for the transition metals Mo and Nb with a high density of states at the Fermi level. For Si under pressure, we found that this scheme has the same degree of convergency as those used here. Furthermore, the calculation by Yin<sup>27</sup> showed that the test of the Hedin-Lunqvist's exchange and correlation functional<sup>30</sup> varies the transition pressure from 149 to 113 kbar. From these facts, the prediction of the transition pressure from  $\beta$ -Sn to sh sensitively depends on the calculational schemes.

The sh phase is calculated to transform into the hcp structure at 410 kbar. Experimentally, the hcp phase is found to be stable at around 400 kbar,<sup>5,7</sup> and this pressure is close to the calculated value. The present result is in better agreement with experiment than another calculated value of 469 kbar.<sup>27</sup> Moriarty and McMahan<sup>9</sup> extrapolated the Yin and Cohen's  $E(V)$  curves<sup>8</sup> and obtained the pressure of 410 kbar for the  $\beta$ -Sn to hcp transition. Our calculation found the pressure for this transition to be 360 kbar.

Actually, a new Si-VI phase was reported to appear above 360 kbar before the transition into the hcp phase.<sup>5</sup> As yet, this new phase has not been identified either experimentally or theoretically. There are several possible conjectures<sup>31</sup> for the structure at pressures between 360 and 400 kbar; a mixture of Si-V (sh), Si-VI, and Si-VII (hcp), different stacking of hexagonal layers including sh and hcp sequences, and structures intermediate between sh

and hcp. To understand the Si-VI phase, we have calculated the total energy barrier from sh to hcp for several volumes between the two transition volumes for the sh and hcp structures. Figure 3 shows the energy differences for intermediate states from the sh phase as a function of displacement for volumes of 11.855, 11.484, and 11.114  $\text{\AA}^3$  per atom. The sh and hcp structures correspond to displacements of one hexagonal base of zero and  $a/\sqrt{3}$  along the [110] direction, respectively. For each intermediate state, the  $c/a$  ratio is optimized. Near the transition volume for the hcp structure, the barrier is found to be small. The decrease of the barrier due to a compression results from a soft phonon mode for the sh phase (this will be discussed later). Then, the sh phase can easily transform into the hcp phase. This behavior is similar to the transition to orthorhombic phase for GaAs due to a soft transverse acoustic mode.<sup>32</sup> Figure 3 shows a local minimum in the total energy change for a volume of 11.114  $\text{\AA}^3$  per atom. While it is not possible as yet to interpret the Si-VI phase, a small energy barrier from sh to hcp suggests that any structure formed by displacements of hexagonal planes, for example, stacking of sh and hcp structures or intermediate phases between sh and hcp, does not cost much structural energy.

At extremely high pressures of the order of Mbar, our calculations indicate that the hcp phase will transform into the fcc phase. This transition was first suggested by Moriarty and McMahan.<sup>9</sup> Our calculated pressure of 1.2 Mbar is somewhat higher than their result of 760 to 820 kbar. However, both calculations are in good agreement for the transition volumes.

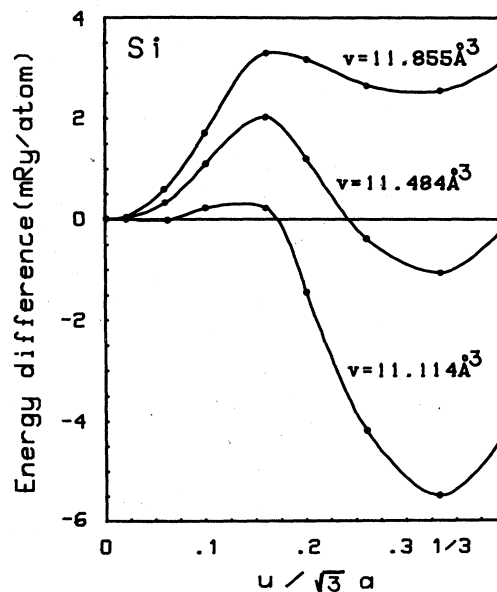


FIG. 3. Energy barriers from the sh to the hcp structures for volumes of 11.855, 11.484, and 11.114  $\text{\AA}^3$  per atom. The sh and hcp phases corresponds to displacements of zero and  $a/\sqrt{3}$ , respectively. The total energies at intermediate states are optimized by a variation of  $c/a$ .

As shown in Fig. 2, the hcp phase of Si is lower in energy than the bcc phase for volumes less than  $0.8V_0$ , where  $V_0$  is the equilibrium volume for the diamond phase. This behavior differs from a previous result<sup>8</sup> where the bcc Si had lower energy for volumes above about  $0.67V_0$ . A fixed value of  $c/a$  for the hcp phase used in this calculation was found to overestimate the total energy by 0.7 mRy/atom. Furthermore, a smaller set of  $k$  points used for the bcc structure underestimates the total energy by 0.7 mRy/atom. These effects cause the bcc phase to be lower in energy than the hcp phase. For the comparison of hexagonal and cubic diamond structures, the cubic diamond structure is stable with respect to the hexagonal structure over a wide range of compressed volume. This behavior is consistent with Yin and Cohen's results. By using a larger number of  $k$  points (28 for CD and 27 points for HD) samples in the irreducible Brillouin zone, the energy difference between two structures at the equilibrium volume is found to be 0.7 mRy/atom which is smaller than their results of 1.6 mRy/atom. These differences are at the limits of the accuracy of these calculations at this time.

The calculated transition volumes are listed in Table I. The transition volumes, 0.707 ( $\beta$ -Sn) and 0.692 (sh) for the  $\beta$ -Sn to sh and 0.596 (sh) and 0.549 (hcp) for sh to hcp transformations, are in good agreement with the measured values.<sup>5,6</sup> The  $c/a$  ratios are estimated to be 0.551 for  $\beta$ -Sn at a volume of  $16 \text{ \AA}^3/\text{atom}$ , 0.955 for sh at  $13.5 \text{ \AA}^3/\text{atom}$ , and 1.695 for hcp at  $11.1 \text{ \AA}^3/\text{atom}$ . In Table II the agreement with the experimental values of 0.552 ( $\beta$ -Sn), 0.94 (sh), and 1.698 (hcp) is also excellent.

It was demonstrated that the Ewald energy plays a dominant role in determining the equilibrium axial ratio.<sup>8</sup> For the  $\beta$ -Sn phase of Si and Ge, the axial ratio of 0.55 obtained from the minimum Ewald energy in Ref. 8 has been found to agree well with the experimental value of 0.552. Figure 4 shows the Ewald energy as a function of the axial ratio for the sh phase of Si. The axial ratio for the minimum Ewald energy is 0.928 and this ratio is close to the measured values of 0.936–0.947.<sup>5–7</sup> In Sn alloys<sup>10</sup> with the sh structure, the  $c/a$  ratio was found to lie between 0.927 and 0.931. Pseudopotential calculations<sup>33</sup> for the Sn alloys showed that the Ewald energy has a minimum for a  $c/a$  of 0.928. This is equivalent to our estimate for  $c/a$  using the *ab initio* pseudopotential method in a monoatomic system. Therefore, the Ewald energy also gives a reasonable estimate of the axial ratio for the sh phase of Si.

TABLE II. Comparisons of the  $c/a$  ratio for  $\beta$ -Sn, sh, and hcp Si with experiment.

	$\beta$ -Sn	sh	hcp
Calculation	0.551	0.955	1.695
Experiment	0.550 <sup>a</sup>	0.936 <sup>a</sup>	1.64 <sup>a</sup>
	0.554 <sup>b</sup>	0.937 <sup>c</sup>	1.698 <sup>c</sup>
		0.947 <sup>c</sup>	

<sup>a</sup>Reference 7.

<sup>b</sup>Reference 34.

<sup>c</sup>Reference 5.

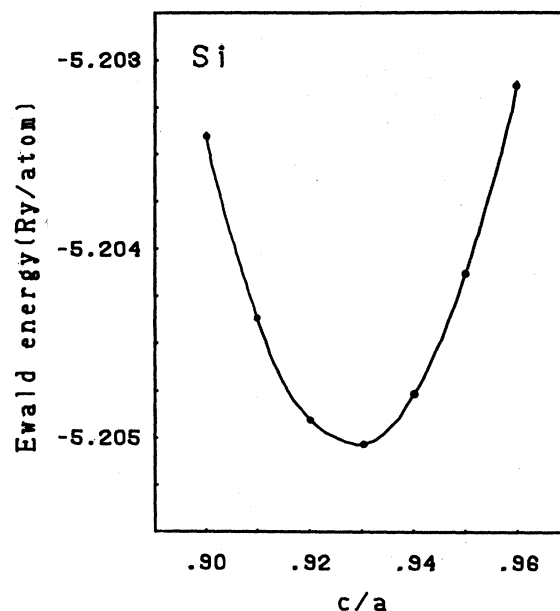


FIG. 4. Ewald energy vs the axial ratio for the sh phase of Si. A volume of  $12.596 \text{ \AA}^3$  per atom is chosen.

#### B. Soft phonon modes for the $\beta$ -Sn and simple hexagonal phases

It is of interest to investigate the phonon modes for the  $\beta$ -Sn, sh, and hcp phases. We have found that the physical origin of solid-solid transition sequence  $\beta$ -Sn  $\rightarrow$  sh  $\rightarrow$  hcp could be understood by examining the pressure-sensitive soft phonon modes. The sh and hcp structures are viewed as phonon displacements with large amplitudes from the  $\beta$ -Sn and sh structures, respectively, accompanied by a change of the  $c/a$  ratio. Figure 1 shows the structural relationships between  $\beta$ -Sn and sh, and between sh and hcp phases.

The sh structure can be determined from  $\beta$ -Sn by displacing one of two interpenetrating body-centered tetragonal sublattices in the direction of the  $c$  axis by  $c/4$ , followed by a slight modification of the interatomic distances. For  $\beta$ -Sn, the ratio of the tetragonal axis is  $1:1:c/a$ , where  $c/a=0.551$  is used. When  $\beta$ -Sn transforms into sh, the  $c$  axis of  $\beta$ -Sn becomes the  $a$  axis of sh. After a displacement of  $c/4$ , the orthorhombic lattice with a ratio of  $1:a/c:a/2c$  needs a modification of the atomic spacings to be the sh phase ( $1:\sqrt{3}:c/a$ ), where  $c/a$  for sh is 0.955. The displacement of tetragonal sublattices corresponds to the longitudinal optic (LO) phonon mode for  $\beta$ -Sn at the zone center ( $\Gamma$ ) in the  $[001]$  direction. Figure 1 shows the polarization for this mode. The calculated phonon frequency for the LO( $\Gamma$ ) mode is 4.19 THz at a volume of  $14.448 \text{ \AA}^3/\text{atom}$ . As the volume is compressed, the LO( $\Gamma$ ) mode becomes softer and the frequency is 3.81 THz for a volume of  $14.078 \text{ \AA}^3/\text{atom}$ .

When a displacement for the LO( $\Gamma$ ) mode changes from zero to  $c/4$  with the  $c/a$  ratio for the  $\beta$ -Sn phase fixed, the total energy is found to increase smoothly.

Then, the energy barriers are found to be 2.3 and 1.9 mRy/atom for volumes of 14.226 and 13.840 Å<sup>3</sup> per atom, respectively, which are close to the transition volumes for the  $\beta$ -Sn and sh phases. In fact, an accurate calculation for the energy barrier from  $\beta$ -Sn to sh is difficult since four parameters (three lattice constants and a displacement) have to be modified until the total energy becomes minimum. However, a variation of  $c/a$  at intermediate stages is found to reduce effectively the energy barrier. We found that the energy change is negative, i.e., no barrier, for a volume of 13.840 Å<sup>3</sup>/atom whereas for a volume of 14.226 Å<sup>3</sup> it is reduced to 0.5 mRy/atom.

The softness of the LO( $\Gamma$ ) mode for  $\beta$ -Sn Si results from bond bending. This was also found in a recent study by Needs and Martin.<sup>28</sup> For other modes at the  $M[00q_{\max}]$  point in the Brillouin zone, the polarizations are determined in the same way as those used for the modes at the  $X[00q_{\max}]$  point in Si and Ge.<sup>20</sup> As shown in Table III the frequency of the transverse optic (TO) mode is about three times larger compared to those for the transverse acoustic and longitudinal modes. Here, the longitudinal optic and acoustic (LOA) modes are degenerate at the  $M$  point. Since the TO mode is effectively equivalent to the compression of the bond, a distortion costs a large energy. For Sn with the  $\beta$ -Sn structure, the TA and LOA modes were also found to be soft.<sup>35</sup>

As shown in Fig. 1, the hcp structure can be formed from the sh phase by sliding one hexagonal plane with respect to the next by  $a/\sqrt{3}$  in the  $[110]$  direction, accompanied by a modification of the  $c/a$  ratio. This displacement corresponds to a transverse acoustic (TA) phonon mode for the sh phase at the  $A[00q_{\max}]$  point in the Brillouin zone. Within the harmonic approximation, this phonon frequency is equivalent to that obtained from displacements along the  $[100]$  axis by symmetry. Table III shows that those frequencies are almost the same at a volume of 13.366 Å<sup>3</sup> (pressure of 180 kbar). A discrepancy for two transverse modes at a pressure of 366 kbar near the transition into the hcp structure results from anharmonic effects. The transverse mode at the  $A$  point is relatively softer than the longitudinal one. As pressure increases, the LA frequency increases while the TA decreases. At higher pressure above 400 kbar, we found that the transverse frequency is imaginary and thus this mode destabilizes the sh phase. This results from the negative pressure dependence of the TA mode. As a consequence, the sh structure can easily transform into the hcp phase. On the other hand, the hcp structure has opposite behavior to the sh phase. At 300 kbar, the transverse mode for the hcp phase in the  $[00q_{\max}]$  direction has an imaginary frequency. Thus, the hcp phase is unstable with respect to the sh structure. However, a compression increases the stability of the hcp structure as shown in Fig. 3.

The Brillouin zone of the hcp structure is about one-half of the sh phase since the  $c$  axis is approximately twice as large and the number of atoms per unit cell is two while the sh phase has only one. In addition, the phonon dispersion along  $\Gamma A$  for the hcp structure can be approximated by folding back the  $\Gamma A$  axis of the sh phase. The optic modes for the hcp phase correspond to the

TABLE III. Calculated phonon frequencies for  $\beta$ -Sn, sh, and hcp Si. Units are in THz and kbar for frequency and pressure, respectively. Displacements along  $+[001]$  and  $*[110]$  directions.

Structure	Mode	Frequency	Pressure
$\beta$ -Sn	LO( $\Gamma$ )	4.19	95
		3.81	110
	TO( $M$ )	12.76	110
	TA( $M$ )	4.12	110
	LOA( $M$ )	4.83	110
Simple hexagonal	LA( $A$ )	12.58	180
		16.61	366
	TA( $A$ ) <sup>+</sup>	3.85	180
		3.57	366
	TA( $A$ ) <sup>*</sup>	3.82	180
Hexagonal close packed		3.24	366
	LO( $\Gamma$ )	17.22	465
		19.15	630
	TO( $\Gamma$ )	4.30	465
		5.21	630
	LOA( $A$ )	11.46	465
		12.54	630
	TOA( $A$ )	4.02	465
		4.69	630

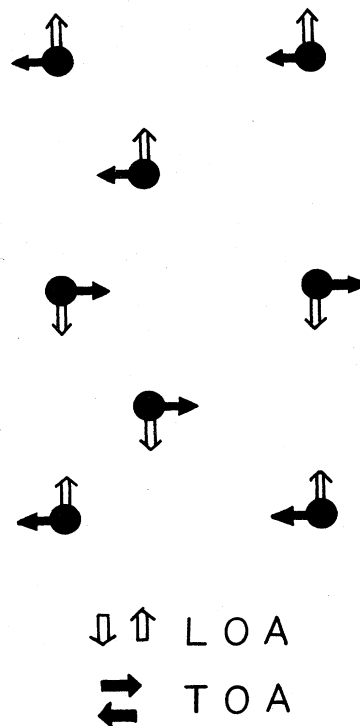


FIG. 5. Phonon polarizations in the  $[11\bar{2}0]$  plane for the longitudinal (LOA) and transverse (TOA) modes at the  $A[00q_{\max}]$  point for the hcp structure.

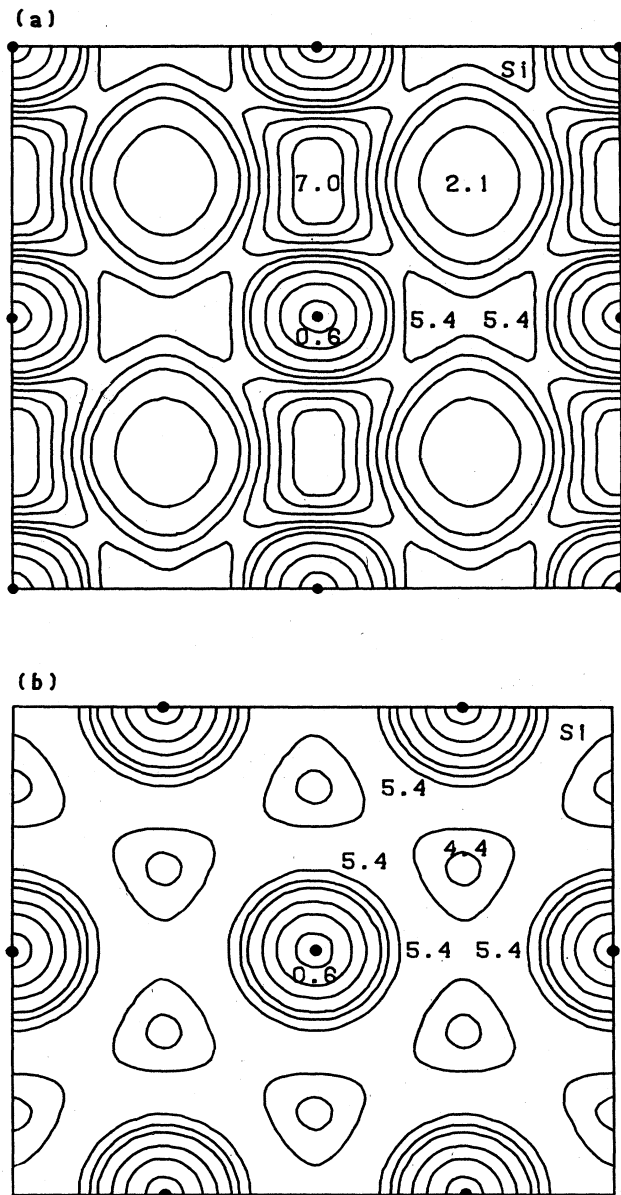


FIG. 6. Charge density contour plots (in units of electrons/cell volume) in the (a)  $[10\bar{1}0]$  and (b)  $[0001]$  planes for the sh phase at a volume of  $12.6 \text{ \AA}^3$  per atom.

folded-back acoustic modes of the sh phase. Then, the LA and TA modes at the  $A$  point for sh will be the  $\text{LO}(\Gamma)$  and  $\text{TO}(\Gamma)$  modes for hcp, respectively. In Table III, the corresponding frequencies are given. When the frequencies at 366 kbar for sh and at 465 kbar for hcp are compared, the  $\text{LO}(\Gamma)$  and  $\text{TO}(\Gamma)$  modes for hcp are very close to the  $\text{LA}(A)$  and  $\text{TA}(A)$  modes for sh, respectively. Slight differences come from the use of different volumes, different ratios for  $c/a$ , and different positions of the second atom in the unit cell. In Fig. 5, the polarizations

for the longitudinal and transverse modes at the  $A$   $[00q_{\text{max}}]$  point in the Brillouin zone are shown. At this point, the optic and acoustic modes are degenerate for each longitudinal and transverse direction.

The calculated charge density for the sh phase shows a large pileup of covalent charge along the axial direction in Fig. 6. The fact that the  $c/a$  ratio is less than 1 suggests that a covalent pile up of charge density might exist. This character is opposite to that of the graphite structure with weak bonding between layers. Hence, the distortion along the interlayer axis produces a stronger restoring force than that in the plane, and thus the LA frequency is higher.

#### IV. CONCLUSION

We have shown that the pseudopotential-total-energy methods produce successfully the transition sequence cubic diamond  $\rightarrow \beta\text{-Sn} \rightarrow \text{sh} \rightarrow \text{hcp} \rightarrow \text{fcc}$  in condensed Si. The successive transitions from  $\beta\text{-Sn}$  to sh to hcp can be viewed as arising from phonon displacements corresponding to the longitudinal optic mode for the  $\beta\text{-Sn}$  and transverse acoustic mode for the sh structures, respectively, in the  $[001]$  direction. These phonon modes have decreasing frequencies with increasing pressure. We have found that the soft phonon modes and a modification of the  $c/a$  ratio reduce effectively the energy barriers from  $\beta\text{-Sn}$  to sh and from sh to hcp, and thus these are likely the origin of the phase transitions.

At this point, the crystal structure of the Si-VI phase has not been clearly established. The present calculations, however, indicate that an intermediate state from the sh to hcp structures has a total energy close to those of the sh and hcp structures. Because of the softness of the transverse mode for the sh phase, a stacking fault in the hexagonal planes of the sh structure might be close to the sh and hcp in the total energy.

Finally, the densities of states (DOS) for the  $\beta\text{-Sn}$ , sh, and hcp phases are found to be fairly high compared to that of normal metals. The calculated DOS's are 4.8, 5.0, and 4.0 states/(Ry atom) for  $\beta\text{-Sn}$ , sh, and hcp Si, respectively. The existence of superconductivity<sup>36</sup> in the  $\beta\text{-Sn}$  phase has been reported earlier with a critical temperature of 6.7 K. We have found that the soft phonon modes and the covalent character remaining in the bonding are likely to be associated with the superconductivity for condensed Si in the  $\beta\text{-Sn}$ , sh, and hcp structures. Details of the electron-phonon interaction and the superconductivity for these phases will appear elsewhere.<sup>16</sup>

#### ACKNOWLEDGMENTS

We would like to thank H. Olijnyk and M. M. Dacorogna for helpful communications. This work was supported by National Science Foundation under Grant No. DMR-83-19024 and by the Director, Office of Energy Research, Office of Basic Energy Sciences, Materials Sciences Division of the U.S. Department of Energy, under Contract No. DE-AC03-76SF00098.

- <sup>1</sup>M. L. Cohen, *Phys. Scr. T* **1**, 5 (1982).
- <sup>2</sup>A. Jayaraman, *Rev. Mod. Phys.* **55**, 65 (1983); *Sci. Am.* **250**, 54 (1984).
- <sup>3</sup>S. Monomura and H. G. Drickamer, *J. Phys. Chem. Solids* **23**, 451 (1962).
- <sup>4</sup>G. J. Piermarini and S. Block, *Rev. Sci. Instrum.* **46**, 973 (1975); W. A. Weinstein and G. J. Piermarini, *Phys. Rev. B* **12**, 1172 (1975).
- <sup>5</sup>H. Olijnyk, S. K. Sikka, and W. B. Holzapfel, *Phys. Lett.* **103A**, 137 (1984).
- <sup>6</sup>J. Z. Hu and I. L. Spain, *Solid State Commun.* **51**, 263 (1984).
- <sup>7</sup>C. S. Mononi, J. Z. Hu, and I. L. Spain, *Phys. Rev. B* (to be published).
- <sup>8</sup>M. T. Yin and M. L. Cohen, *Phys. Rev. B* **26**, 5668 (1982).
- <sup>9</sup>A. K. McMahan and J. A. Moriarity, *Phys. Rev. B* **27**, 3235 (1983).
- <sup>10</sup>G. V. Raynor and J. A. Lee, *Acta. Metall.* **2**, 616 (1954).
- <sup>11</sup>B. C. Giessen, *Adv. X-Ray Anal.* **12**, 111 (1969).
- <sup>12</sup>S. Froyen and M. L. Cohen, *Phys. Rev. B* **28**, 3258 (1983).
- <sup>13</sup>M. T. Yin and M. L. Cohen, *Phys. Rev. B* **29**, 6996 (1984).
- <sup>14</sup>K. J. Chang and M. L. Cohen, *Phys. Rev. B* **30**, 5376 (1984).
- <sup>15</sup>K. J. Chang and M. L. Cohen (unpublished).
- <sup>16</sup>M. M. Dacorogna, K. J. Chang, and M. L. Cohen, *Bull. Am. Phys. Soc.* **30**, 569 (1985); and unpublished.
- <sup>17</sup>E. Wigner, *Trans. Faraday Soc.* **34**, 678 (1938).
- <sup>18</sup>S. Froyen and M. L. Cohen, *Phys. Rev. B* **29**, 3770 (1984).
- <sup>19</sup>K. J. Chang and M. L. Cohen, *Phys. Rev. B* **30**, 4774 (1984).
- <sup>20</sup>M. T. Yin and M. L. Cohen, *Phys. Rev. B* **26**, 3259 (1982).
- <sup>21</sup>P. K. Lam and M. L. Cohen, *Phys. Rev. B* **27**, 5986 (1983).
- <sup>22</sup>P. K. Lam, M. Y. Chou, and M. L. Cohen, *J. Phys. C* **17**, 2065 (1984).
- <sup>23</sup>D. R. Hamann, M. Schlüter, and C. Chiang, *Phys. Rev. Lett.* **43**, 1494 (1979).
- <sup>24</sup>J. Ihm, A. Zunger, and M. L. Cohen, *J. Phys. C* **12**, 4401 (1979).
- <sup>25</sup>C. L. Fu and K. M. Ho, *Phys. Rev. B* **28**, 5480 (1983).
- <sup>26</sup>F. D. Murnaghan, *Proc. Nat. Acad. Sci. U.S.A.* **30**, 244 (1944).
- <sup>27</sup>M. T. Yin, in *Proceedings of the 17th International Conference on the Physics of Semiconductors, San Francisco, 1984* (unpublished).
- <sup>28</sup>R. Needs and R. Martin, *Phys. Rev. B* **30**, 5390 (1984).
- <sup>29</sup>R. Jeanloz, private communication.
- <sup>30</sup>L. Hedin and B. I. Lundqvist, *J. Phys. C* **4**, 2064 (1971).
- <sup>31</sup>H. Olijnyk, private communication.
- <sup>32</sup>K. Kunc and R. M. Martin, *Phys. Rev. B* **24**, 2311 (1981).
- <sup>33</sup>D. Weaire and A. R. Williams, *Philos. Mag.* **19**, 1105 (1969).
- <sup>34</sup>J. Jamieson, *Science* **139**, 762 (1963).
- <sup>35</sup>J. M. Rowe, *Phys. Rev.* **163**, 547 (1967).
- <sup>36</sup>J. Wittig, *Z. Phys.* **195**, 215 (1966).